Quantum Superposition of Target and Product States in Reactive Electron Scattering from CF_4 Revealed through Velocity Slice Imaging

Frímann H. Ómarsson,[1] Ewelina Szymanska,[2] Nigel J. Mason,[2] E. Krishnakumar,[3] and Oddur Ingólfsson[1,*]

[1]*Department of Chemistry and Science Institute, University of Iceland, Dunhaga 3, 107 Reykjavík, Iceland*

[2]*Department of Physical Sciences, The Open University, Walton Hall, MK7 6AA Milton Keynes, United Kingdom*

[3]*Tata Institute of Fundamental Research, Homi Bhabha Road, Colaba, Mumbai 400005, India*

(Received 8 April 2013; published 6 August 2013)

Exploiting the technique of velocity slice imaging, we have performed a detailed study of reactive electron scattering with CF_4. We have measured the electron impact energy dependence of both the angular and kinetic energy distributions of the channels yielding F^- and CF_3^- anions. These data provide an unprecedented insight into the quantum superposition of the target state and product channels, respectively, of T_d and C_{3v} symmetry, and shed new light on the dissociation dynamics.

DOI: 10.1103/PhysRevLett.111.063201 PACS numbers: 34.80.Ht

In molecules with a highly symmetrical configuration of the nuclei, the electronic term may be degenerate, and hence it is possible to find nuclear displacements that lift the degeneracy and reduce the point symmetry. Under such circumstances, the minima in the adiabatic potentials correspond to a finite number (>1) or even a continuous set of nuclear configurations. Thus, it becomes impossible to describe the state of the molecule by assuming that the nuclei are fixed at a certain position of equilibrium corresponding to one particular minimum in the adiabatic potential. For a molecule with a threefold or higher symmetry, this phenomenon is described by the Jahn-Teller effect (JTE) [1], but a similar effect is observed when breaking lower symmetries, such as in the case of CO_2 [2,3]. The dynamics induced by this effect are related to electrical and magnetic properties of molecular systems, and there are many illustrations of the JTE in spectroscopic studies. However, in contrast, less is known about its consequences in scattering studies, despite the fact that, e.g., in low energy electron scattering of gas phase molecular targets, the angular distributions of the final products are dictated by the symmetry of the resonance states involved. In this context, Ziesel *et al.* [4] inferred that in a very low energy (< 0.1 eV) electron collision with CCl_4, the *s*-wave attachment is enabled through lowering of the symmetry of the target from T_d to C_{3v}. Similarly, in C_6H_6, the nuclear distortion caused by the JTE lowers the symmetry of the molecule and thus allows the *s* wave to ''leak in'' to form a symmetry allowed virtual state [5–7]. Furthermore, in a recent dissociative electron attachment (DEA) study on CH_4, the JTE is proposed to be reflected in the angular distribution of the H^- ions [8]. It has therefore been proposed that, in general, in the scattering dynamics of a low energy projectile interacting with highly symmetric molecular targets, the description of the scattering processes within a single (rigid) point group is inadequate [5,9,10]. DEA is such a process, where an incident electron is captured by the molecular target (*ABC*) in a low energy (< 10 eV), reactive scattering process, to form a transient negative ion (TNI), i.e., a resonance ($ABC^{-\#}$). In DEA, this resonance subsequently decays to produce a negative ion fragment and a neutral counterpart:

$$e^- + ABC \rightarrow ABC^{-\#} \rightarrow AB + C^-. \quad (1)$$

Thus, in DEA, characteristic features of both the initial target and the TNI may be reflected in the angular distribution and kinetic energy release of the respective fragments. It should be noted that generally the TNI may also decay in to the elastic or inelastic channel by reemission of the electron, and the whole scattering process is a superposition of these three channels.

In this Letter, we have studied DEA to carbon tetrafluoride CF_4, which in its ground state is tetrahedral, i.e., of T_d symmetry, and therefore is a very suitable model compound to study the fundamental aspects of electron-molecule interactions such as the coupling between electronic states and nuclear motion. The outer valence electron configuration of CF_4 is $\ldots(4a_1)^2(3t_2)^6(1e)^4(4t_2)^6(1t_1)^6$, leading to a $^1A_1$ ground state. The two lowest virtual orbitals in CF_4 are expected to be the $5a_1$ and $5t_2$ antibonding σ^* orbitals; however, their relative positions are not well established (see, for example, Refs. [11,12] and references therein). In electron attachment to CF_4 in its undistorted T_d symmetry, we expect the formation of a shape resonance of either A_1 or T_2 symmetry, or a core excited resonance of E, T_2, or T_1 symmetry. However, upon electron attachment to the triply degenerate t_2 orbital, the molecular anion is expected to assume C_{3v} symmetry, by stretching one of the C-F bonds, and thus the triply degenerate t_2 orbital will split into a nondegenerate a_1 and a doubly degenerate e orbital [11]. We therefore explored whether such degeneracy can be observed in the DEA products, resulting from reactive electron scattering from this target. In the current measurements, we use the velocity slice imaging (VSI) technique [13], where angular distributions can be recorded over the whole angular range 0°–360° simultaneously.

The experimental setup has been described previously [13]. In brief, it consists of a molecular beam crossed with a magnetically collimated, pulsed electron beam, a time of flight mass spectrometer operating in a VSI configuration, and a phosphor screen detector with pulsed bias and a CCD camera. After electron-molecule collisions, the product anion cloud expands for 200 ns to form a Newton sphere. Using this method, we can obtain angular distributions of the fragment anions directly, without having to use a reconstruction algorithm such as the inverse Abel transformation. Such distributions may then be fitted using the method described by Azria *et al.* [14], which is a polyatomic extension of the diatomic model originally proposed by O'Malley and Taylor [15] and later modified by Tronc *et al.* [16]. Details of the theory behind the fitting procedure and its application can be found in these references and more specifically in Refs. [8,17].

In Fig. 1, velocity slice images for the F^- ions are shown at incident energies of 5.0 and 7.5 eV and for the CF_3^- ions at incident energies of 5.5 and 8.5 eV. Angular distributions in DEA are symmetric about the electron momentum axis, which passes down through the center of the distributions in Fig. 1, and therefore we fitted the angular distributions over the range from 0°–180°; these fits are shown in Fig. 2. The angular distributions for F^- and CF_3^- are approximately mirror images with respect to the vertical axis, confirming that these anions are produced via the same resonance. These angular distributions can only be reproduced satisfactorily if contributions from both the T_d and the C_{3v} point groups are considered. This is also apparent in a recent VSI study on CF_4 [18], where the CF_3^- angular distribution was fitted within a single symmetry T_d point group, but s-wave contributions were included in these fits to achieve acceptable agreement. We note that in the description of resonant electron scattering by molecules within the T_d point group, such s-wave contributions are not allowed [19]. Using a single symmetry T_d point group, the current fits to the F^- and CF_3^- angular distributions result in R^2 values below 0.89 and 0.68, respectively (dashed lines in Fig. 2). In contrast, fits considering contributions from both the T_d and the C_{3v} point group, by using a linear combination of these, show R^2 values in excess of 0.96 for both fragments (solid lines in Fig. 2). Even though the difference is more apparent for CF_3^-, it should be noted that the extreme angular values, describing the forward and backward (0° and 180°) components, are also fitted considerably better for F^- using the two point-group fit method. We further note that such forward or backward asymmetry can arise when there is more than one partial wave contribution, where at least one is even and another one odd, and their coherent action gives an odd function for the intensity. Here, for the T_2 symmetry within the T_d point group alone, we have p, d, and f waves.

We can explain these results by a quantum mechanical superposition of the T_d and C_{3v} states in the scattering process, requiring a dynamic description of the scattering event. Because of the lifting of the degeneracy of electronic

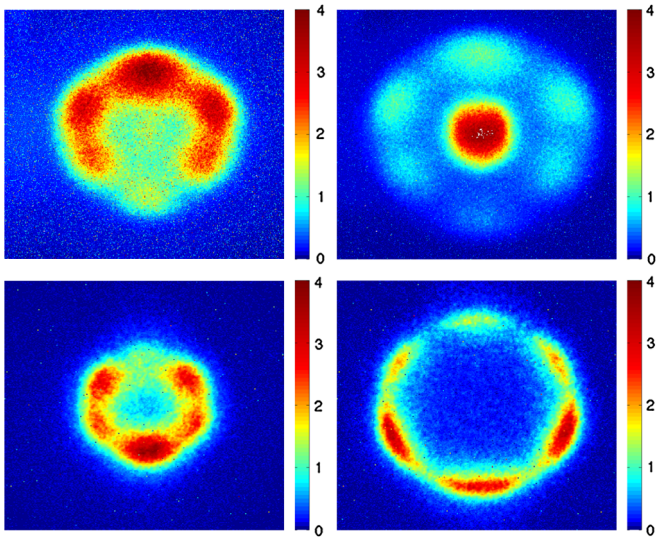

FIG. 1 (color online). Velocity slice images of F^- (upper) at 5.5 eV (left) and 7.5 eV (right) and of CF_3^- (lower) at 5.5 eV (left) and 8.5 eV (right). The electron beam traverses downward and through the center of each figure.

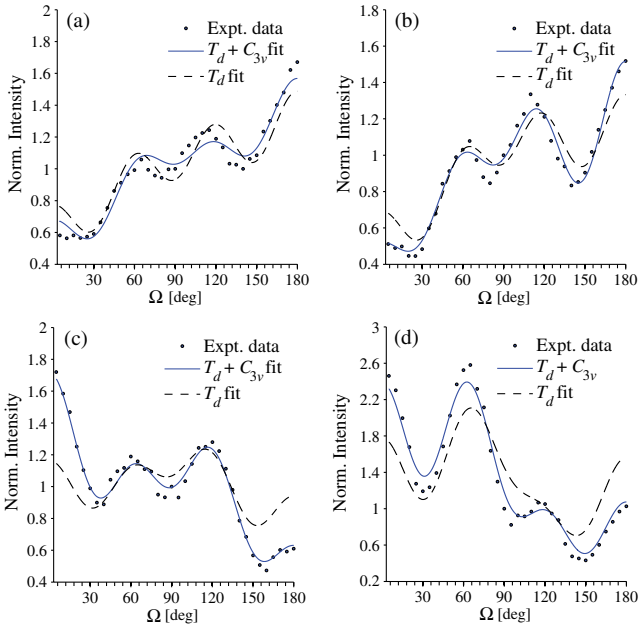

FIG. 2 (color online). Fitted angular distribution for F^- (upper panel) at (a) 5.5 eV and at (b) 7.5 eV and for CF_3^- (lower panel) at (c) 5.5 eV and at (d) 8.5 eV. The dotted lines show fits using a single symmetry T_d point group, and the solid lines are fits using a linear combination of contributions from both the T_d and C_{3v} point groups. The former give an R^2 value of <0.89 and <0.68 for F^- and CF_3^-, respectively, while the latter give R^2 values in excess of 0.96 in all cases. In particular the fits, using a single symmetry T_d point group, fail to reproduce the angular distribution around 0° and 180°.

states, the incoming electron interacts with both the T_d configuration and the C_{3v} configuration, when forming the resonance. This is subsequently reflected in the angular distribution of the anionic fragments produced by the decay of the resonance. Thus, any description of the scattering process within a single symmetry group fails, as the resulting angular distributions can no longer be described within the framework of a static scattering center using a single symmetry group. We attribute this to the fast nuclear separation, caused by the lifting of the degeneracy of the triply degenerate t_2 orbital not allowing the angular distribution of the anionic fragments to be depicted within the single T_d point group describing the initial symmetry of the molecule.

This is also manifested in the kinetic energy release (KER) arising from the dissociative relaxation of this resonance. Figure 3 shows the KER for (a) the F^- and (b) the CF_3^- fragmentation channel, i.e., the total kinetic energy that is released in the respective fragmentation processes. The KER in the F^- channel shows a monotonic rise with increasing electron energy with a slope of 0.4, which corresponds to 40% of the available excess energy being released into the kinetic energy of the fragments. In contrast, the plot of the KER through the CF_3^- channel shows two distinct sections discernible in the electron energy dependency. For the first, below 7 eV, the slope is about 0.6, but for the second, above 7 eV, the slope is close to unity. Hence, the CF_3^- formation proceeds through two distinct processes with the majority of the available excess energy transferred into KER above 7 eV. This is also evident from the different kinetic energy distributions in the CF_3^- ion yield, which is about 0.2 eV narrower (FWHM), for the forward component, at 8.5 eV than at 5.5 eV. Hence, above 7 eV, where the bulk of the excess energy goes into KER, the distribution is narrower than

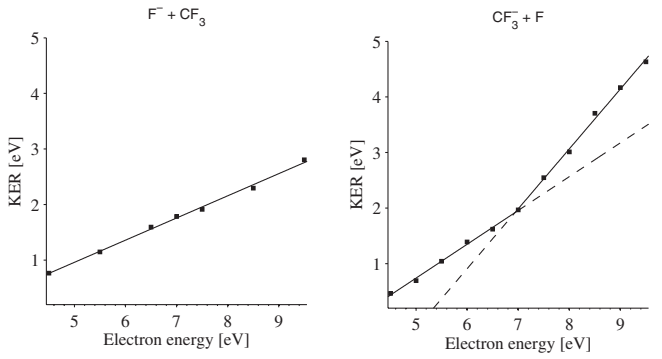

FIG. 3. Measured KER versus incident electron energy for the F^- channel (left) and the CF_3^- channel (right). While the KER in the F^- channel shows a monotonic rise with increasing incident electron energy, two distinct sections are clearly discernable in the CF_3^- channel. From these, the KER in the higher energy section is close to unity; i.e., all excess energy goes into the kinetic energy of the fragments.

below 7 eV, where part of the excess energy goes into internal excitation and thus causes the kinetic energy distribution to broaden. We note at this point that earlier KER measurements using time of flight did not reveal these distinctive components [20,21].

We attribute these two components in the CF_3^- KER, to thermochemical restrictions of the DEA leading to internal vibrational redistribution (IVR) when this process proceeds at electron incident energies below the F_3C-F bond dissociation energy (BDE). In contrast, at electron incident energies above the F_3C-F BDE, these restrictions do not apply, and strong coupling of the electronic and nuclear kinetic energy is clearly manifested in the substantially higher KER. For a "simple" DEA process, e.g., the CF_3^- formation from CF_4, the thermochemical threshold is given by the difference between the BDE of the F_3C-F bond and the adiabatic electron affinity of the CF_3 radical; see Eq. (1). Accordingly, if the incident electron energy is less than the F_3C-F BDE, i.e., <5.67 eV, the nascent CF_3^- product anion has to relax toward its equilibrium C_s geometry for molecular dissociation to occur (see Fig. 4, pathway 1). Hence, at incident energies below the F_3C-F BDE, a contribution from the adiabatic electron affinity is needed in order to make the reaction thermochemically possible.

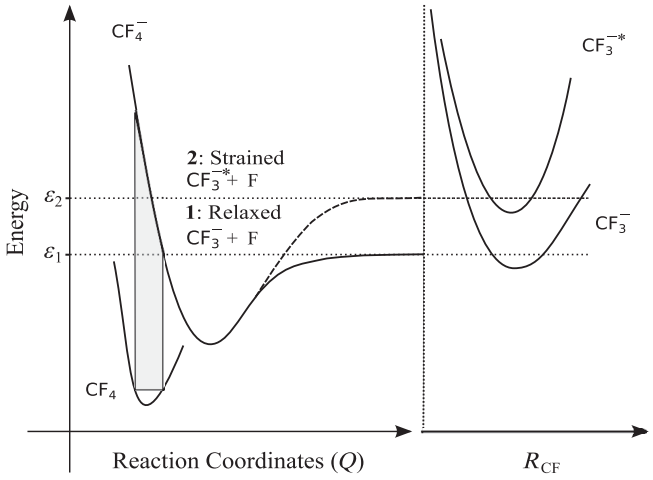

FIG. 4. Schematic representation of dissociation pathways yielding the relaxed CF_3^- **1** and the strained (unrelaxed) CF_3^{-*} **2** in DEA to CF_4. The reaction paths are depicted on the left along a reaction coordinate Q. For the relaxed CF_3^- formation (solid lines), this reaction coordinate represents the F_3C-F bond elongation as well as relaxation of the FCF angles toward the CF_3^- equilibrium geometry. For CF_3^{-*} (dashed line), on the other hand, this reaction coordinate represents the F_3C-F bond elongation only. The shaded area represents the Franck-Condon transition from the neutral ground state to the anionic potential energy surface, and ϵ_1 and ϵ_2 the thermochemical threshold for reaction pathways 1 and 2, respectively. On the right-hand side, the schematic potential energy curves of CF_3^- and CF_3^{-*} are given as a function of R_{CF}, i.e., equal elongation of all C-F bonds.

This, in turn, restricts and slows down the nuclear separation and thus promotes IVR of the available excess energy at the cost of the KER. However, if the incident electron energy is larger than the F_3C-F *BDE*, dissociation can proceed in a quasidiatomic manner, without relaxation, and CF_3^- can be formed in an excited (geometrically unrelaxed) state: CF_3^{-*} (pathway 2 in Fig. 4).

This in turn allows for rapid conversion of electronic kinetic energy into nuclear kinetic energy and thus unrestricted separation without substantial IVR, resulting in substantially higher KER in the process.

This interpretation is further supported when we compare the difference between the thresholds for the CF_3^- and CF_3^{-*} formations we derive from our current study with a recent theoretical study on DEA to CF_3 by Hayashi [22], where he calculated the potential energy surfaces for CF_3, CF_3^-, and CF_3^{-*} as a function of the CF distance. In his study, the FCF angle was fixed at the 111° equilibrium angle of the neutral radical for both CF_3 and CF_3^{-*} and at the 99.8° equilibrium angle of the ground state anion for CF_3^-. The total energy was then explored along a coordinate of equal stretching of all C-F bonds, hence, under C_{3v} symmetry constraints. The minimum total energy of CF_3^- was found to be 1.72 eV below that of the neutral radical, in good agreement with the electron affinity of CF_3 [23]. In contrast, for CF_3^{-*}, the minimum total energy was found to be about 0.5 eV below that of the neutral radical, i.e., about 1.2 eV above the geometrically relaxed CF_3^- anion. At the threshold for a given DEA process, the ions are formed with zero kinetic energy and the threshold energy, E_{th} can thus be obtained from the current data by extrapolating the electron energy dependency of the KER to zero kinetic energy. With this method, we obtain a threshold of 3.79 and 5.11 eV for the formation of CF_3^- below 7 eV and CF_3^{-*} above 7 eV, respectively. This is a difference of 1.32 eV, which compares well with the value of about 1.2 eV derived in the calculations by Hayashi [22].

Hence, at incident electron energies below the F_3C-F BDE, the momentum of the nuclear separation is damped, due to the required relaxation of the product CF_3^-. This restricts the fast nuclear separation expected from the strong electronic and nuclear coupling responsible for the JTE, and thus leads to increased IVR. In contrast, above the F_3C-F BDE, the TNI (or "resonance" CF_4^-) can respond instantaneously to the changing electronic configuration, and the F_3C-F bond dissociation can proceed in a quasidiatomic manner. This contrast leads to a clear manifestation of strong electronic and nuclear coupling in the substantial KER increase in the CF_3^- formation above about 7 eV.

In contrast, F^- formation is very different from that for the CF_3^- formation, as no geometry change is necessary for the 3.40 eV electron affinity of fluorine to be available over the whole width of this resonance. Thus, the incident electron energy dependence of the KER in the F^- channel shows a monotonic rise over the whole width of this resonance.

In summary, by using the new approach of VSI to study the reactive scattering process of DEA to CF_4, we have shown that the quantum superposition of the target and product states, respectively of T_d and C_{3v} symmetry, is clearly manifested in the angular distributions of the product anionic fragments, hence making it impracticable to describe such a distribution within a single T_d point group of the target's initial symmetry. Furthermore, the different KER in the CF_3^- formation above and below about 7 eV reveals fast conversion of electron kinetic energy into nuclear kinetic energy provided through the lifting of the degeneracy of the t_2 LUMO in this system, i.e., the JTE in this scattering process.

F. H. Ó. acknowledges grants for short-term scientific missions to Milton Keynes from the two COST actions CM0601 (ECCL) and CM0805 (Chemical cosmos) as well as support from the Eimskip University Fund. O. I. acknowledges financial support from the Icelandic Center for Research (RANNÍS). E. K. acknowledges a Marie Curie Fellowship. E. S. and N. J. M. acknowledge support from the EU FPVII Marie Curie Programme. The authors would like to thank Dr. N. Bhargava Ram for help with the data analysis and Professor David Field for fruitful discussions during the preparation of this manuscript.

*Corresponding author.
odduring@hi.is

[1] G. Herzberg, *Molecular Spectra and Molecular Structure* (Van Nostrand, New York, 1966).
[2] L. A. Morgan, Phys. Rev. Lett. **80**, 1873 (1998).
[3] D. Field, N. C. Jones, S. L. Lunt, and J. P. Ziesel, Phys. Rev. A **64**, 022708 (2001).
[4] J. P. Ziesel, N. C. Jones, D. Field, and L. B. Madsen, Phys. Rev. Lett. **90**, 083201 (2003).
[5] G. A. Gallup, Phys. Rev. A **34**, 2746 (1986).
[6] G. A. Gallup, J. Chem. Phys. **99**, 827 (1993).
[7] D. Field, J. P. Ziesel, S. L. Lunt, R. Parthasarathy, L. Suess, S. B. Hill, F. B. Dunning, R. R. Lucchese, and F. A. Gianturco, J. Phys. B **34**, 4371 (2001).
[8] N. B. Ram and E. Krishnakumar, Chem. Phys. Lett. **511**, 22 (2011).
[9] S. F. Wong and G. J. Schulz, Phys. Rev. Lett. **35**, 1429 (1975).
[10] N. C. Jones, D. Field, J. P. Ziesel, and T. A. Field, J. Chem. Phys. **122**, 074301 (2005).
[11] S. I. Itoh, S. Tanaka, and Y. Kayanuma, Phys. Rev. A **60**, 4488 (1999).
[12] E. H. Bjarnason, F. H. Ómarsson, M. Hoshino, H. Tanaka, M. J. Brunger, P. Limão-Vieira, and O. Ingólfsson, Int. J. Mass Spectrom. **339–340**, 45 (2013).
[13] D. Nandi, V. S. Prabhudesai, E. Krishnakumar, and A. Chatterjee, Rev. Sci. Instrum. **76**, 053107 (2005).
[14] R. Azria, Y. Le Coat, G. Lefevre, and D. Simon, J. Phys. B **12**, 679 (1979).

[15] T. F. O'Malley and H. S. Taylor, Phys. Rev. **176**, 207 (1968).
[16] M. Tronc, C. Schermann, R. I. Hall, and F. Fiquet-Fayard, J. Phys. B **10**, 305 (1977).
[17] F. H. Ómarsson, O. Ingólfsson, N. J. Mason, and E. Krishnakumar, Eur. Phys. J. D **66**, 51 (2012).
[18] L. Xia, X.-J. Zeng, H.-K. Li, B. Wu, and S. X. Tian, Angew. Chem., Int. Ed. **52**, 1013 (2013).
[19] F. H. Read, J. Phys. B **1**, 893 (1968).
[20] E. Illenberger, Chem. Phys. Lett. **80**, 153 (1981).
[21] Y. Le Coat, J. Ziesel, and J. Guillotin, J. Phys. B **27**, 965 (1994).
[22] D. Hayashi, Jpn. J. Appl. Phys. **43**, 2711 (2004).
[23] H.-J. Deyerl, L. S. Alconcel, and R. E. Continetti, J. Phys. Chem. A **105**, 552 (2001).